Parallel Fast Multipole Boundary Element Method for Crustal Dynamics

Leonardo Quevedo, Gabriele Morra, R. Dietmar Müller

The University of Sydney, School of Geosciences, EarthByte Group.
Madsen Building F09, The University of Sydney, NSW, 2006

E-mail: Leonardo.Quevedo@sydney.edu.au, Gabriele.Morra@sydney.edu.au, d.muller@usyd.edu.au

Abstract. Crustal faults and sharp material transitions in the crust are usually represented as triangulated surfaces in structural geological models. The complex range of volumes separating such surfaces is typically three-dimensionally meshed in order to solve equations that describe crustal deformation with the finite-difference (FD) or finite-element (FEM) methods. We show here how the Boundary Element Method, combined with the Multipole approach, can revolutionise the calculation of stress and strain, solving the problem of computational scalability from reservoir to basin scales. The Fast Multipole Boundary Element Method (Fast BEM) tackles the difficulty of handling the intricate volume meshes and high resolution of crustal data that has put classical Finite 3D approaches in a performance crisis. The two main performance enhancements of this method: the reduction of required mesh elements from cubic to quadratic with linear size and linear-logarithmic runtime; achieve a reduction of memory and runtime requirements allowing the treatment of a new scale of geodynamic models. This approach was recently tested and applied in a series of papers by [2, 3, 4] for regional and global geodynamics, using KD trees for fast identification of near and far-field interacting elements, and MPI parallelised code on distributed memory architectures, and is now in active development for crustal dynamics. As the method is based on a free-surface, it allows easy data transfer to geological visualisation tools where only changes in boundaries and material properties are required as input parameters. In addition, easy volume mesh sampling of physical quantities enables direct integration with existing FD/FEM code.

1. Introduction

Geodynamic modelling is facing the challenge of dealing with ever increasing resolution data on kinematic, topographic and material features of the Earth. Crustal deformation has been traditionally studied by using Finite Difference (FD) and Finite Element Methods (FEM) on models fitting such constraints, but the inherent 3 dimensional character of the physical system, its associated complex composite rheologies, as well as its planetary scale that spans very large variations in viscosity has taken this approaches to their limit.

We propose the Fast Multipole (FM) extension to the Boundary Element Method[1] (BEM) as the novel numerical method that is better suited for plate tectonics modelling involving processes at planetary scales [2, 3, 4]. The FM-BEM speedup and low memory requirements derived from the use of 3 dimensional analytical solutions defined only on the surface of the regions of

[1] A general reference for FM-BEM is [1]

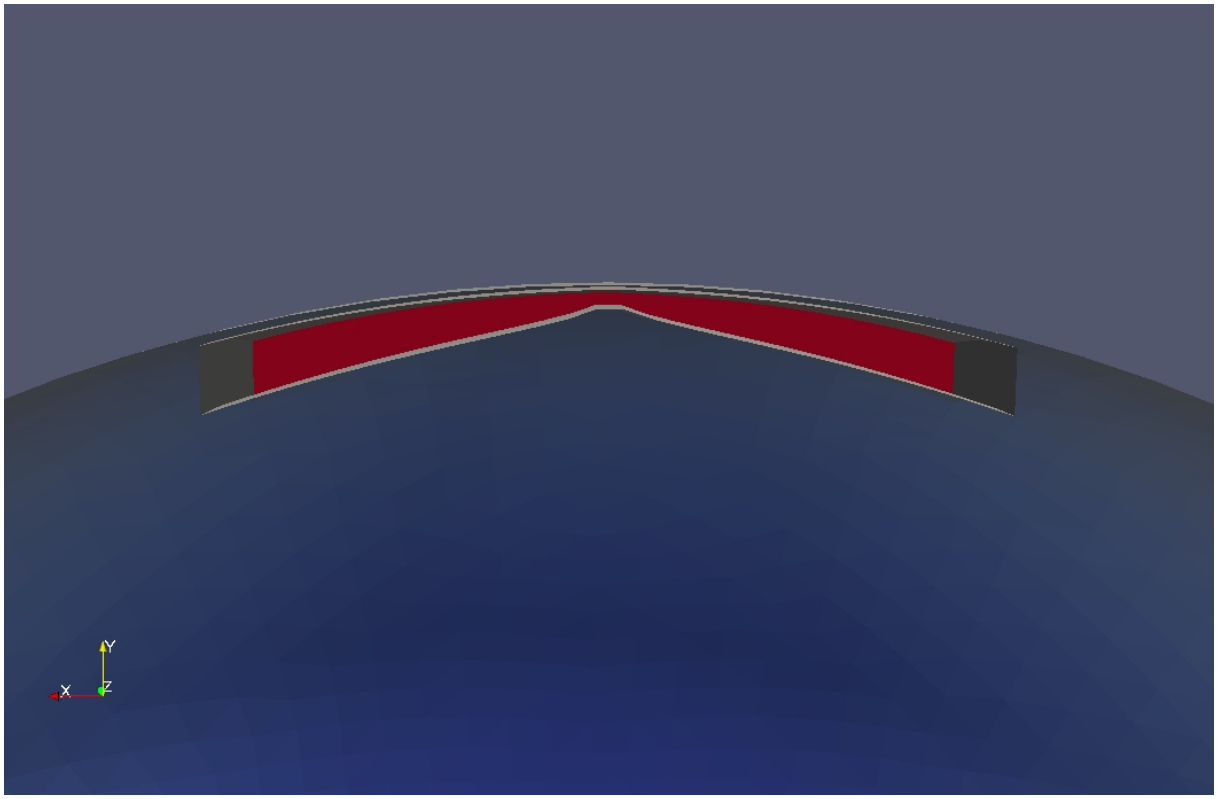

Figure 1. Initial state of the model

interest, allows solving on bigger and finer meshes in a more convenient lower dimensionality. This suits more ambitious solutions to problems where global structures like the 10000 km wide Pacific Plate are to be strongly coupled to small scale dynamics such as trench fault lubrication occurring in 1-100 m thick lithospheric shear-zones [5]. Such improvement in performance opens the door to effectively model such multiscale problems self-consistently, that is to let the system follow fundamental forces like gravity in an unconstrained fashion, and reproduce the measured quantities by tuning the unknown driving forces like slab pull, ridge push or mantle drag.

This paper is structured as follows. In section 2, we describe the geodynamical model, the methodology of the solution and its governing equations. In section 3 we describe the FM-BEM applied to the physical model, and in section 4 we summarise the results and present the scaling behaviour of the solver on the number of processors.

2. Physical Model

Our initial configuration consists of a surface delimiting a region of lithosphere with the shape of a Mid Ocean Ridge immersed in a spherical Earth as shown in figure 1. Following a self-consistent approach, we obtain the stable ridge configuration and its associated stress map, assuming strictly the presence of fundamental forces:

(i) Buoyancy difference between the lithosphere, the overlying air/water layer, and the underlying mantle.

(ii) Viscous resistance of the mantle to lithospheric motion.

(iii) Resistance of the lithosphere to bending and stretching.

The buoyancy difference arising from the density difference between the lithosphere and its surroundings is a critical property as it prevents the plate from sinking straight down [6]. The

mantle exerts a drag force on the lithosphere that controls the spreading rate by tuning energy dissipation. In our simplified model the strength of the oceanic lithosphere remains constant with a viscosity two orders of magnitude larger than that of the mantle.

The model is bootstrapped from an extrapolation of the 2 dimensional analytical solution of oceanic lithospheric cooling [7]. Subsequently, the free-surface of the Earth is dynamically adapted on top of the resulting lithospheric topography at each step to a depth of half of the lithospheric thickness. This method is shown to create a physically consistent buoyancy force for a plate [2] where the mantle–ocean density difference self-consistently sustains lithosphere and allows free deformation of its upper surface, leading to oceanic topography. This requires the introduction of a critical distance h_{crit} parameter between the boundary elements of Earth and lithospheric surfaces. A low value of this parameter results in instabilities during numerical computation, a high value leads to inaccuracies in the calculation of the uplifting force.

After obtaining an equilibrium configuration of the physical system where the characteristic ridge shape is obtained and the spreading process starts, the displacement field is sampled in a 3 dimensional grid containing the region of interest. From this data the resulting stress field is inferred.

2.1. Boundary Integral Formulation of Stokes Flow

Steady highly viscous flow governing the dynamics of the system is described by the Stokes equation

$$\nabla \cdot \boldsymbol{\sigma} + \rho \mathbf{b} = 0 \tag{1}$$

where $\mathbf{b}$ represents the body forces and σ_{ij} is the full stress tensor with positive tension. Constitutive equations for viscous deformations can be written in terms of the strain rate tensor $\dot{\boldsymbol{\varepsilon}}$ as

$$\dot{\varepsilon}_{ij} \equiv \frac{1}{2}(v_{i,j} + v_{j,i}) = \frac{1}{2\mu}\sigma_{ij} \tag{2}$$

where v_i represents the velocity field components and μ is the dynamic viscosity.

Following the formulation of [8] one may recast (1) as an integral equation defined in the boundary ∂D of the physical domain D

$$v_j(\mathbf{x}_0) = \frac{1}{8\pi\mu}\int_{\partial D} \sigma_{ik}(\mathbf{x}) n_k G_{ij}(\mathbf{x}, \mathbf{x}_0) dS(\mathbf{x}) + \frac{1}{8\pi}\int_{\partial D} v_i(\mathbf{x}) n_k T_{ijk}(\mathbf{x}, \mathbf{x}_0) dS(\mathbf{x}) \tag{3}$$

where G_{ij} and T_{ijk} are the steady, Green's functions for velocity and traction fields respectively, also known as the *Stokeslet* and the *Stresslet*

$$\begin{aligned} G_{ij}(\mathbf{x} - \mathbf{x}_0) &= \frac{\delta_{ij}}{r} + \frac{\hat{x}_i \hat{x}_j}{r^3}, \\ T_{ijk}(\mathbf{x} - \mathbf{x}_0) &= -6\frac{\hat{x}_i \hat{x}_j \hat{x}_k}{r^5}, \end{aligned} \qquad \text{with} \quad \hat{\mathbf{x}} = \mathbf{x} - \mathbf{x}_0 \quad \text{and} \quad r = |\hat{\mathbf{x}}|. \tag{4}$$

A more appropriate form of the boundary integral equation (3) for multiphase flows in the presence of a gravity field can be found by taking the viscosity of the mantle as a reference value μ_0, defining a relative viscosity $\lambda_i = \mu_i/\mu_0$ and expressing the normal gravitational stress jump induced by the differential density between regions separated by surfaces S_i as

$$\Delta \mathbf{f} = \Delta\rho(\mathbf{b} \cdot \mathbf{x})\mathbf{n}\,, \tag{5}$$

being $\mathbf{n}$ the normal to the surface on the point $\mathbf{x}$. With this, we can obtain the value of the velocity field on the surfaces $\mathbf{x} \in S_i$ from

$$\frac{1+\lambda_i}{2}\mathbf{v}(\mathbf{x}) - \sum_j^N \frac{1-\lambda_j}{8\pi}\int_{S_j}^{PV} \mathbf{n}\cdot\mathsf{T}\cdot\mathbf{v}\,dS = -\frac{1}{8\pi\mu_0}\sum_j^N \int_{S_j} \mathsf{G}\cdot\Delta\mathbf{f}\,dS\,, \tag{6}$$

where PV denotes the principal value of the integral.

2.2. Boundary Integral Formulation of Elasticity
Elastic constitutive equations are defined by

$$\varepsilon_{ij}^{(\text{elastic})} = \frac{1}{2G}\sigma_{ij} - \frac{1}{3K}p\,\delta_{ij}, \tag{7}$$

where G and K are the constant elastic shear and bulk modulus respectively and $p = \frac{1}{3}(\sigma_{11}+\sigma_{22}+\sigma_{33})$ is the pressure. For elastic materials with a Poisson ratio of $\nu = 0.5$ the bulk modulus diverges $K \to \infty$ and one can disregard the second term of the last equation, obtaining a formulation analogous to the viscous one presented in (2). In this case one can use a similar boundary integral (3) to solve the *displacements* u_i in terms of the stress tensor σ_{ij} and the elastic shear, where the Green functions remain identical to the viscous ones.

$$u_j(\mathbf{x}_0) = \frac{1}{8\pi G}\int_{\partial D}\sigma_{ik}(\mathbf{x})n_k G_{ij}(\mathbf{x},\mathbf{x}_0)dS(\mathbf{x}) + \frac{1}{8\pi}\int_{\partial D} u_i(\mathbf{x})n_k T_{ijk}(\mathbf{x},\mathbf{x}_0)dS(\mathbf{x}) \tag{8}$$

In the elastic formulation, one may explore the effects of more complex boundary conditions by simply changing the RHS in the analogous form of (6). This is essential to the simulation of the short time scale dynamics of plate tectonics, where stress field is dominated by the action of interplate and intraplate forces [9, 10]. On the same model that evolves through the million years timescale we have an analogous framework to study instantaneous elastic behaviour. With this boundary method, it is very easy to introduce traction and compressional forces to test the interaction with its surroundings and gauge the effects of tectonic driving forces like slab pull. Once values on the boundary have been established, one can use (3) to find the displacement field everywhere in space, from which the stress field can be directly calculated.

3. Numerical Method

The surfaces S_i and the supported quantities $\mathbf{u}$, $\Delta\mathbf{f}, \ldots$ are discretised into panels which correspond to the elements of a 3 dimensional triangulated mesh shown in figure 2, note that the region surrounding the area of interest has been inhomogeneously refined with respect to the rest of the sphere. The boundary integral equation (6) on the panels becomes the linear system

$$((1+\lambda)/2 + \mathsf{T})\,\mathbf{U} = \mathbf{F}\,. \tag{9}$$

Instead of fully populating the matrix operator in the left hand side of this equation, a procedure that scales quadratically in the number of elements N for both memory requirements and computation time, we use a fast multipole method (FMM)[11, 12, 13] for the evaluation of the integrals in (6). The FMM scales as $N\log(N)$, which is far more tractable for large systems and still allows the use of a Generalised Minimised Residual method (GMRES) or any Krylov space based method that does not rely on the storage of the full matrix.

Multipole methods consist in a controlled approximation of a convolution that is valid when its kernel decays, something which is assured in our case by the nature of Green's functions (4). More explicitly, to compute

$$u(\mathbf{x}_0) = \int_D G(\mathbf{x}_0 - \mathbf{x})\rho(\mathbf{x})dV(\mathbf{x})\,, \tag{10}$$

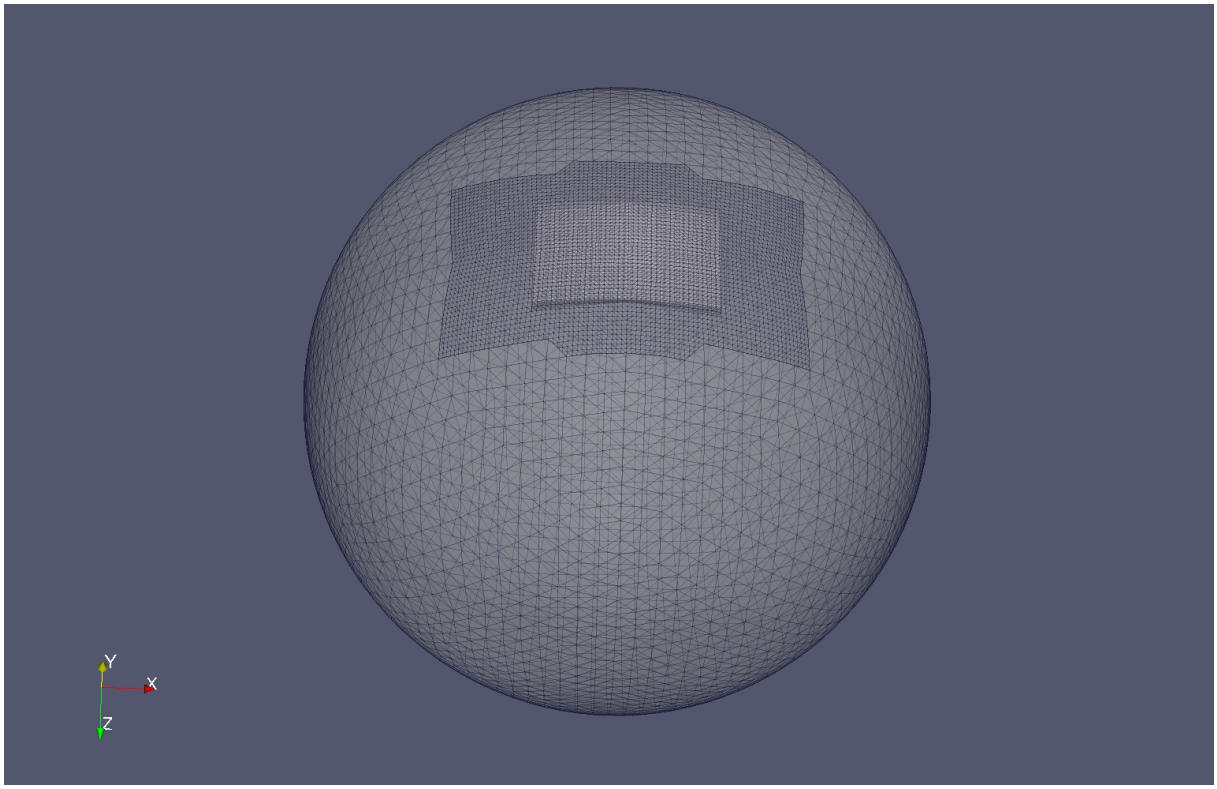

Figure 2. Triangulated mesh of the physical model

we consider the contribution from a subset of the domain $D_i \subset D$, that is far *enough* from our evaluation point $\mathbf{x}_0$ and Taylor expand the kernel G around $\mathbf{x}_c \in D_i$

$$\begin{aligned} u(\mathbf{x}_0) &= \int_{D_i} G(\mathbf{x}_0 - \mathbf{x})\rho(\mathbf{x})dV(\mathbf{x}) \\ &\simeq \int_{D_i} \left(G(\mathbf{x}_0 - \mathbf{x}_c) - \nabla G(\mathbf{x}_0 - \mathbf{x}_c)\cdot(\mathbf{x}_0 - \mathbf{x}_c) + \ldots\right)\rho(\mathbf{x})dV(\mathbf{x}) \\ &\simeq G(\mathbf{x}_0 - \mathbf{x}_c)\int_{D_i}\rho(\mathbf{x})dV(\mathbf{x}) \\ &\quad -\nabla G(\mathbf{x}_0 - \mathbf{x}_c)\cdot\int_{D_i}(\mathbf{x}_0 - \mathbf{x}_c)\rho(\mathbf{x})dV(\mathbf{x}) + \ldots \end{aligned} \tag{11}$$

This expansion involves successive moment integrals of the density distribution in D_i, that is, the *multipoles*. The FMM algorithm sorts the sources in a tree structure whose cells contain the multipoles and carries out a field evaluation through a tree traversal. The desired precision in the approximation of the interactions is determined by a tree traversal stopping criterion based on a prescribed tolerance. The reader is referred to [11, 12, 13] for further details. The present FMM code can handle convolutions with the Green's functions for the Poisson equation, the Stokeslet or the Stresslet, employing up to the second order moments of the source distributions (quadrupoles).

To obtain the stress, the displacement field is sampled in a grid and the second order centred finite difference gradient is calculated. Stress is then derived from the constitutive equations (7).

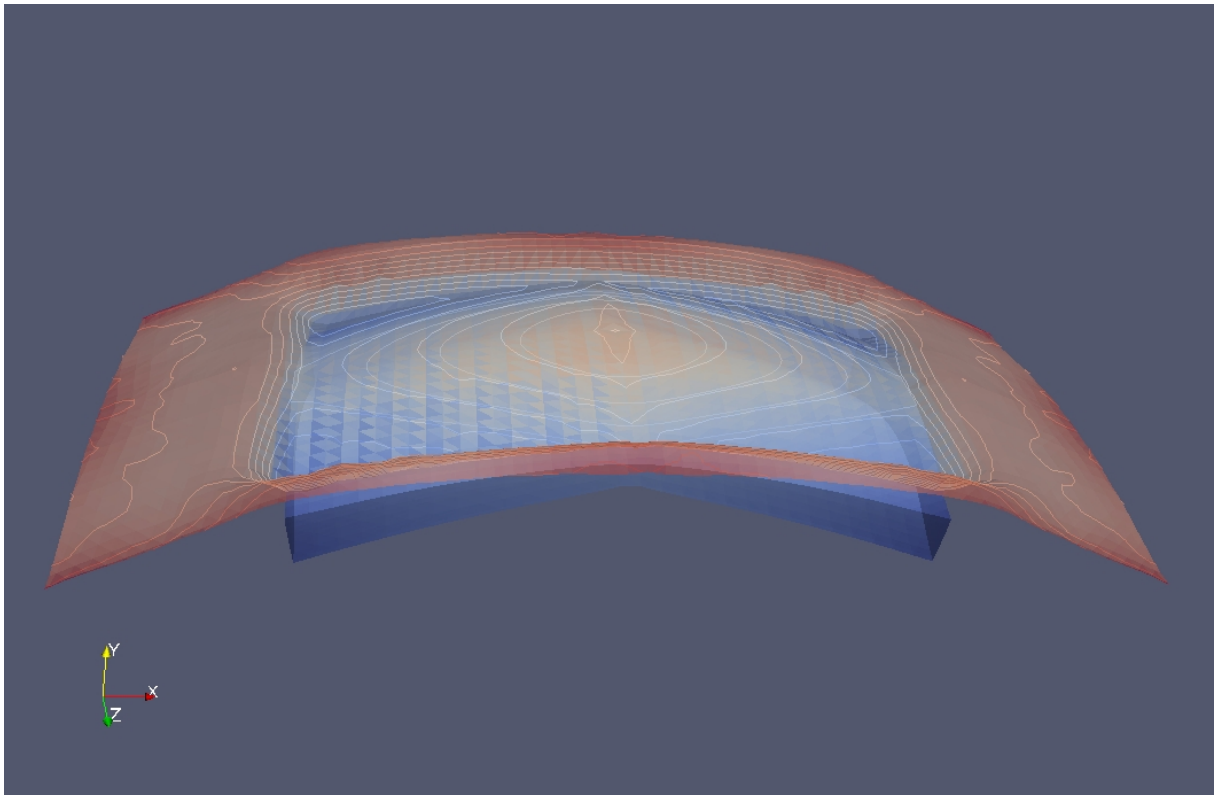

Figure 3. Mid ocean ridge topography emerging from dynamical evolution of lithosphere-mantle-surface interaction

4. Results and Performance

For a lithosphere model with 100 times the viscosity of the mantle, the characteristic ridge topography arises self-consistently in the surface of the Earth as depicted in figure 3. The dynamics begin with a transient regime where the lithosphere sinks and the surface of the Earth adapts to this displacement until the system relaxes from the initial conditions to an equilibrium plateau. In this stable state more realistic topographic and mechanical features arise and may be compared with known data [14, 15].

Instead of proceeding with the Stokes flow simulation, the elastic stresses are studied by changing (3) to the framework where it describes the elastic deformations of the material as described in section 2.2. At this stage it is possible to impose additional boundary conditions to represent any additional force that modifies the state of stress on the plate. The displacement field is sampled in a 3 dimensional region of interest and used to construct a stress map which is shown in figure 4. Though buoyancy suspends the lithosphere in isostasy there is a clear boundary effect on the edges of the plate that have the tendency to subduct.

The total processing time as a function of the number of CPUs is shown on figure 5 shows the parallel efficiency tested on the Silica Science and Engineering High Performance Computing system at The University of Sydney. Silica is a SGI Altix XE1200 Cluster with Infiniband connections in which each computing node has 8 processors. We have taken the maximum load of a node (8 CPUs) as a reference. The shared tree implementation multipole integrals reduces the communication load at the expense of memory requirements. Parallel efficiency is mainly affected by geometrical mesh query and manipulation routines that are currently in process of being parallelised.

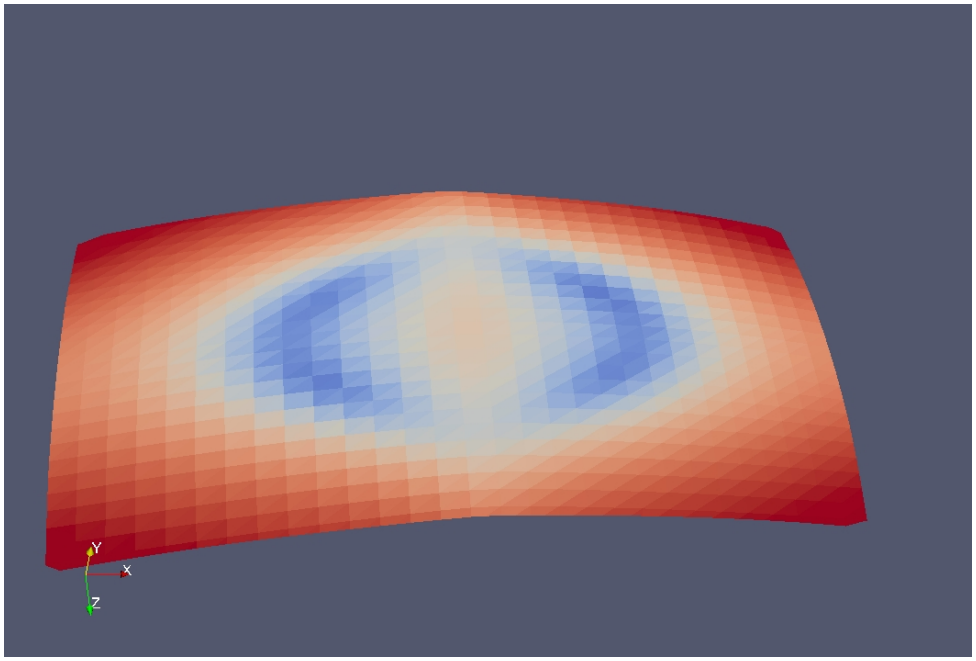

Figure 4. Second stress invariant on the lithosphere surface

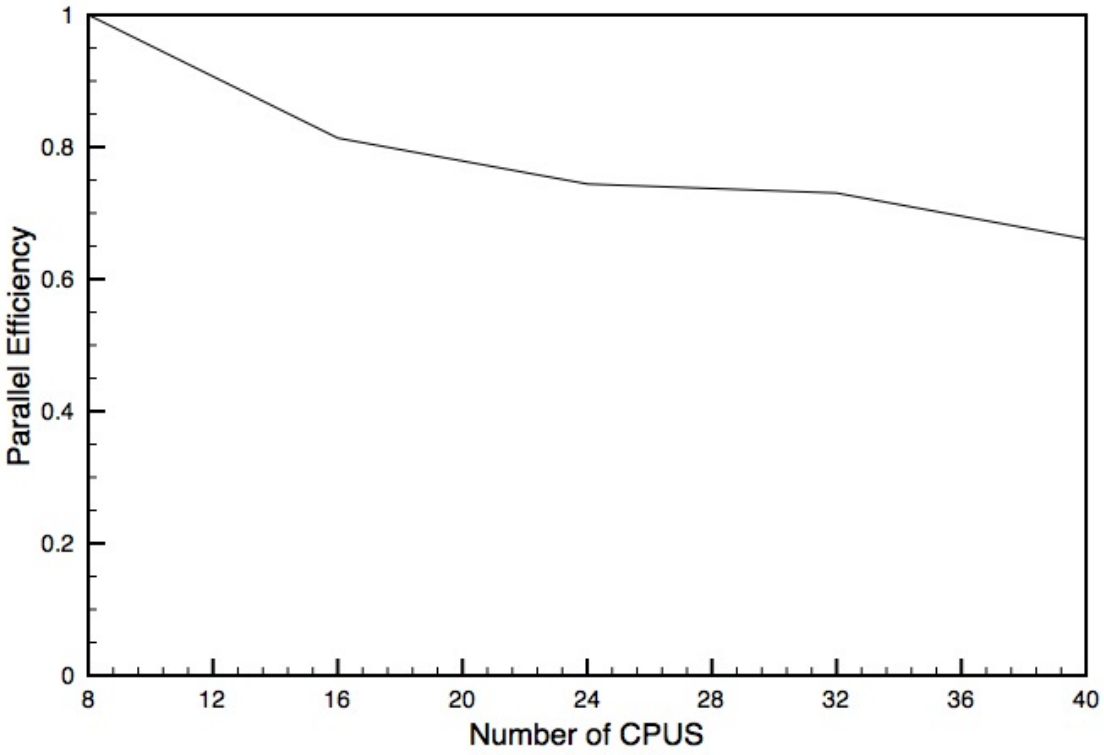

Figure 5. Parallel efficiency a function of the number of CPUs

References

[1] Liu Y 2002 *Fast Multipole Boundary Element Method. Theory and Applications in Engineering* (Cambridge, UK: CUP)

[2] Morra G, Chatelain P, Tackley P and Koumoutsakos P 2007 *Large Scale Three-Dimensional Boundary Element Simulation of Subduction* (*Lecture Notes in Computer Science* vol 4489/2007) (Berlin / Heidelberg: Springer) pp 1122–1129

[3] Morra G, Chatelain P, Tackley P and Koumoutzakos P 2008 *Acta Geotechnica* **4** 95–105

[4] Morra G, Yuen D A, Boschi L, Chatelain P, Koumoutsakos P and Tackley P *Physics of the Earth and Planetary Interiors* in press

[5] Regenauer-Lieb K, and Yuen D A 2003 *Earth-Science Reviews* **63** 295–349

[6] Funiciello F, Morra G, Regenauer-Lieb K and Giardini D 2003 *Journal of Geophysical Research* **108** 2206

[7] Turcotte D L and Schubert G 2009 *Geodynamics* 2nd ed (New York, USA: CUP)

[8] Pozrikidis C 1992 *Boundary Integral and Singularity Methods for Linearized Viscous Flow* (Cambridge, UK: CUP)

[9] Lithgow-Bertelloni C and Guynn J H 2004 *J. Geophys. Res.* **109** B01408

[10] Sandiford M, Wallace M and Coblentz D 2004 *J. Geophys. Res.* **16** 325 – 338

[11] Barnes J and Hut P 1986 *Nature* 324

[12] Greengard L and Rokhlin V 1987 *Journal of Computational Physics A* **73** 325–348

[13] Warren M and Salmon J 1993 *Supercomputing* 12–21

[14] Dick H J B, Lin J and Schouten H 2003 *Nature* **426** 405–412

[15] Ranero C R, Morgan J P, McIntosh K and Reichert C 2003 *Nature* **425** 367–373